

COMMUNICATION

Supplementary Materials

Few-Layered MoN-MnO Heterostructures with Interfacial-O Synergistic Active Centers Boosting Electrocatalytic Hydrogen Evolution

Fei Lin,^a Hongye Qin,^a Xuejie Cao,^a Lei Yang,^a Tongzhou Wang,^a and Lifang Jiao^{*a}

^aKey Laboratory of Advanced Energy Materials Chemistry (Ministry of Education), Renewable Energy Conversion and Storage Center (ReCast), College of Chemistry, Nankai University, Tianjin 300071, China

E-mail: jiaolf@nankai.edu.cn.

Materials and Methods

Synthesis of MoN-MnO: Mn(MoO₄)(H₂O) as the precursor materials was synthesized through a hydrothermal reaction. 0.25 mmol Na₂MoO₄·2H₂O and 0.25 mmol MnCl₂·4H₂O were dissolved in 30 ml distilled (DI) water. And the homogeneous solution including Mo and Mn source was transferred to Teflon autoclaves and the 2×4 cm² Ni foam (NF) also was pitched. The subsequent reaction was placed at 160 °C for 12 h. After drying for 8 h under 50 °C. The precursors were annealed in ammonia atmosphere under 500 °C and hold for 1 h.

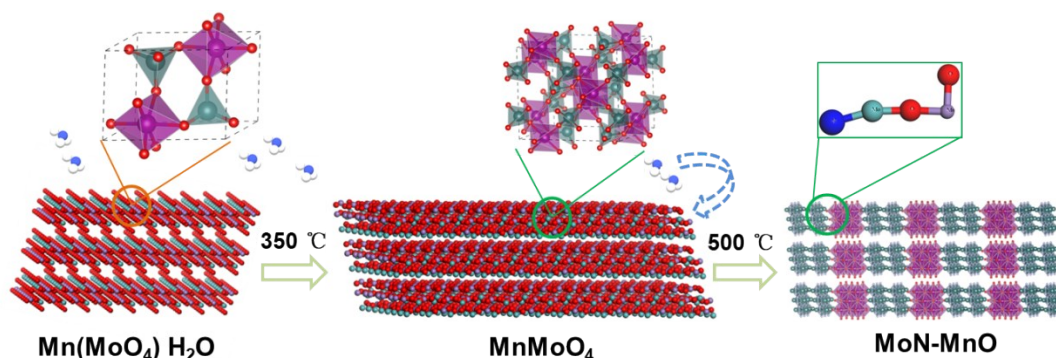
Synthesis of MoN and MnO: MoN was prepared as following reported method [1]. 400 mg Mo powders were dispersed in 40 mL ethanol and stirred for 1h. Subsequently, the 1.2 mL H₂O₂ was injected in it. After 20 h stirring, the dark blue suspension A was obtained. in 3 mL ethanol dissolved 10 mg Co (OCOCH₃)₂ was mixed with A. And it was mixed with 12.8 g NaCl and dried at 50 °C with vigorous stirring. Subsequently, dark blue crystal was annealed to 750 °C for 5 h under NH₃. Finally, the black powder was washed by HCl and deionized water several times to remove the NaCl template and Co and dried in vacuum filtration.

MnO was prepared as following reported method [2]. 100 mg commercial Ketjen Black was dispersed in 100 ml deionized water by 3 h ultrasonic vibration. 100 mg KMnO₄ with 10 mL water was injected into the above suspension solutions, and it was stirred for 12 h at 70 °C. After centrifugation and washing, the black product was obtained. Followed by sintering at 500 °C for 5 h under Ar/10% H₂, the MnO was yielded.

Materials Characterization: Scanning electron microscopy (SEM) was carried out on JEOL JSM-7500F and transmission electron microscopy (TEM) investigations were performed by Talos F200X G2 AEMC instruments. The inductively coupled plasma optical emission spectroscopy (ICP-OES) was carried out on SpectroBlue. Raman test and X-ray photoelectron spectroscopy (XPS) were performed by Renishaw inVia and PHI5000 VersaProbe ESCALAB 250xi, respectively. Etching conditions: an argon ion gun is employed to etch and thin the sample. The size of etching spot was 1.5mm. The etching voltage was 2kV, and the etching rate was 0.05nm/s. And the C 1s was selected in all XPS spectrum.

Electrochemical Measurements: The synthesized MoN-MnO on NF was directly treated as the working electrode after washing with DI water and ethanol. The counter electrode and reference electrode are graphite rod and SCE with salt bridge, respectively. 2mg Pt/C (Pt: 20% mass fraction from Johnson Matthey) was dispersed in 1mL dispersion with water: isopropanol: Nafion =3: 1: 0.1. Subsequently, 0.5 mg Pt/C was loaded on NF as comparison electrocatalyst. The turnover frequency (TOF) is based on that number of active sites from CV curve (-0.2 V-0.6 V vs. RHE, scan rate of 50 mV s⁻¹) in neutral solution (pH=7). While n could be calculated by $n=Q/2F$ (F: Faraday constant; Q: the whole charge of CV curve). Followed by equation, $TOF=I/2Fn$, the TOF could be obtained.

DFT Computational Details: First-principles calculations are performed based on density functional theory (DFT) by Vienna ab initio simulation package (VASP) with Projector Augmented Wave (PAW) method. The Perdew-Burke-Ernzerhof (PBE) functional within the generalized gradient approximation (GGA) is treated as the electronic exchange-correlation energy. The GGA + U method with the U = 3.9 eV for Mn and 4.38eV for Mo. The energy cut-off for the plane-wave basis was set to 500 eV for all calculations. The convergence condition for the geometry optimization is that the maximal force on each atom less than 0.05 eV/Å, and the convergence condition for energy is 10⁻⁵ eV. Six-layered MoN slab model combined with MnO cluster was employed to simulate the interaction surface. Moreover, Antiferromagnetic MnO cluster with lowest energy as our cluster model. All constructions possess larger than 15 Å vacuum region in the z direction to minimize the interaction between planes. 2×2×1 and 4×4×1 Monkhorst-Pack k-point sampling was chosen for geometry optimization, electronic self-consistent calculation, respectively.



Schematic S1. Schematic illustration of the synthetic procedure of MoN-MnO.

As shown in Figure S1, the Mn(MoO₄)(H₂O) is confirmed by the X-ray diffraction (XRD) pattern. In Figure S1b-d, the obtained Mn(MoO₄)(H₂O) nanosheets are verified by scanning electron microscopy (SEM) and transmission electron microscopy (TEM). In Figure S1e-g and enlarged S1b, the few-layered Mn(MoO₄)(H₂O) possesses 5 layers and thickness of 4.8 nm. And the loading mass was 1.35 mg cm⁻² by inductively coupled plasma optical emission spectroscopy (ICP-OES) as shown in Table S1. After the treatment in the NH₃ at 500 °C, the formation mechanism of MoN-MnO is shown in Schematic S1 based on Figure S2-4. The different temperature can influence the process of decomposing. This is evident that the temperature exceeding 400 °C is very necessary to decompose Mn(MoO₄) into MoN-MnO.

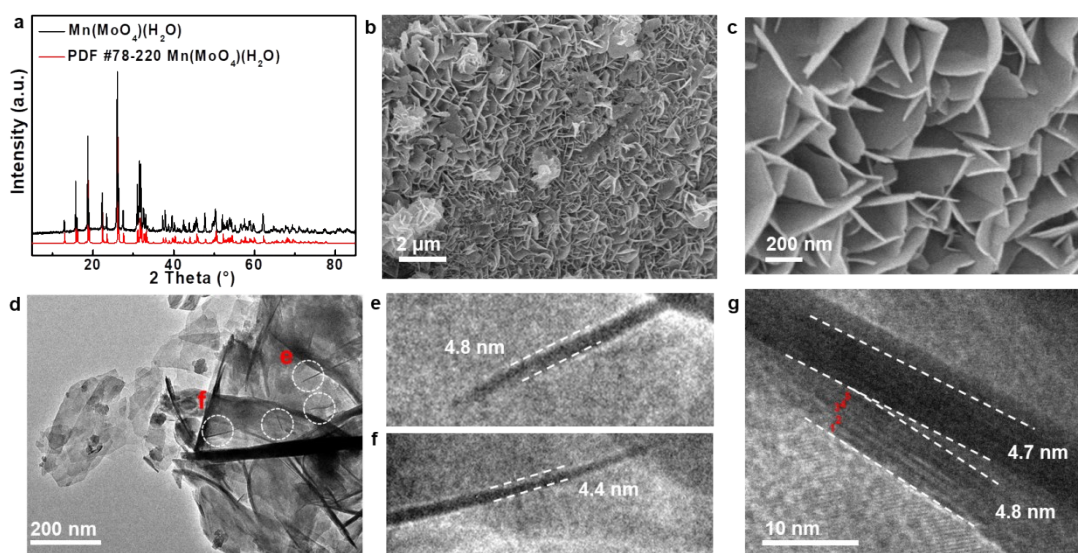


Figure S1. (a) XRD patterns, (b) and (c) SEM image, (d-g) TEM of Mn(MoO₄)(H₂O).

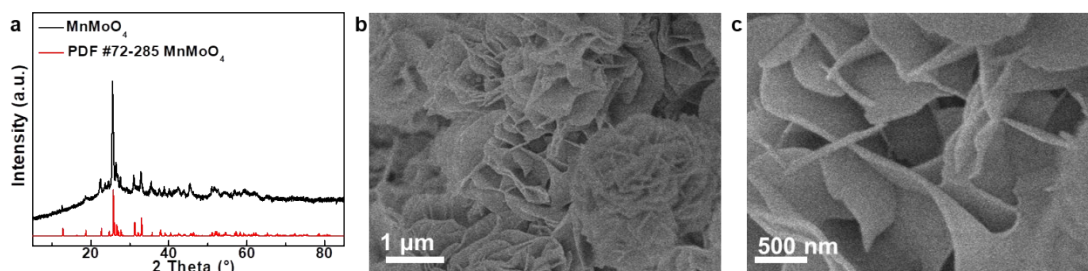


Figure S2. (a) XRD patterns, (b) and (c) SEM image of Mn(MoO₄)(H₂O) calcined in air at 350 °C.

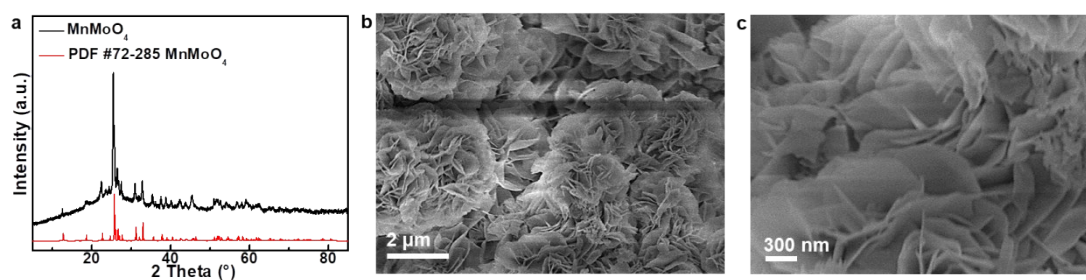


Figure S3. (a) XRD patterns, (b) and (c) SEM image of $\text{Mn}(\text{MoO}_4)(\text{H}_2\text{O})$ calcined in Ar at 350 °C.

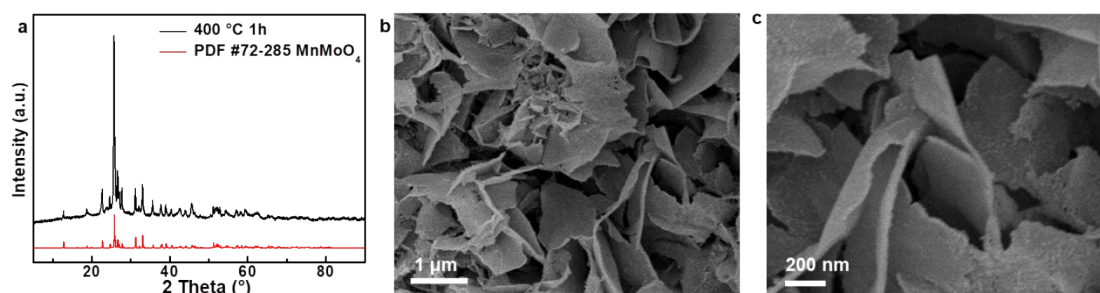


Figure S4. (a) XRD patterns, (b) and (c) SEM image of $\text{Mn}(\text{MoO}_4)(\text{H}_2\text{O})$ calcined in the NH_3 at 400 °C.

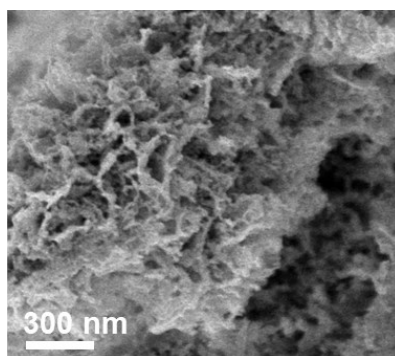


Figure S5. SEM image of $\text{Mn}(\text{MoO}_4)(\text{H}_2\text{O})$ calcined in the NH_3 at 500 °C.

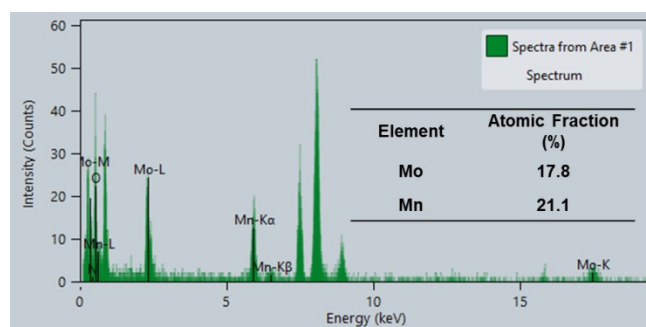


Figure S6. EDX spectrum and of MoN-MnO sample (inset is the atomic ratio of Mo with Mn).

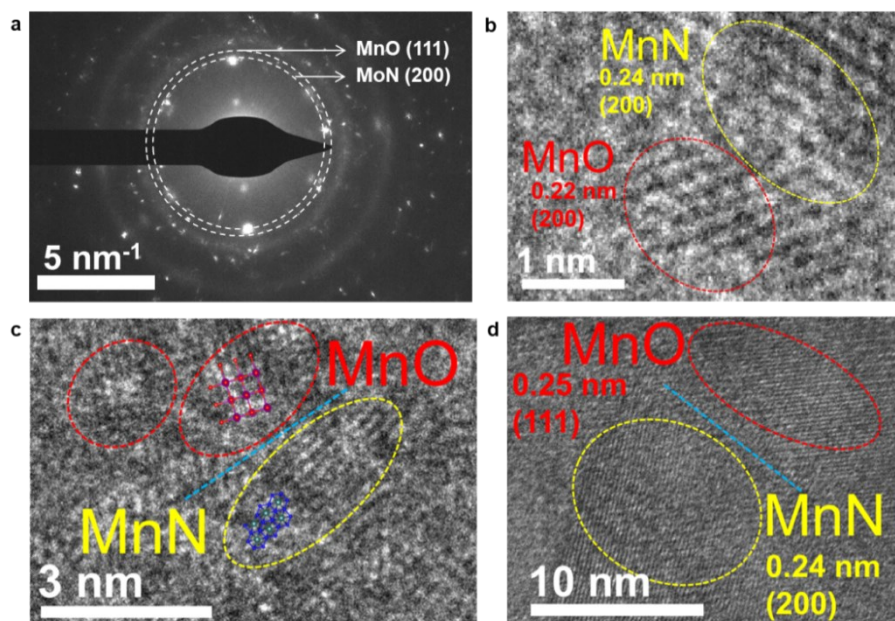


Figure S7. (a) The selected area electron diffraction (SAED) of MoN-MnO. (b) The enlarged of Figure 1h. (c and d) The HRTEM of MoN-MnO.

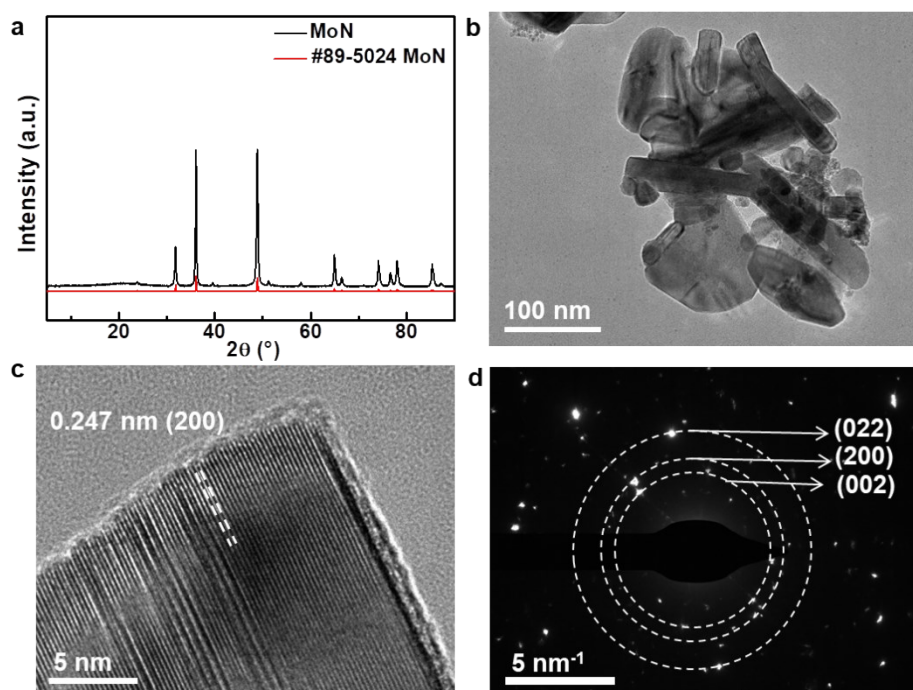


Figure S8. (a) XRD patterns, (b) and (c) TEM image and (d) SAED of MoN.

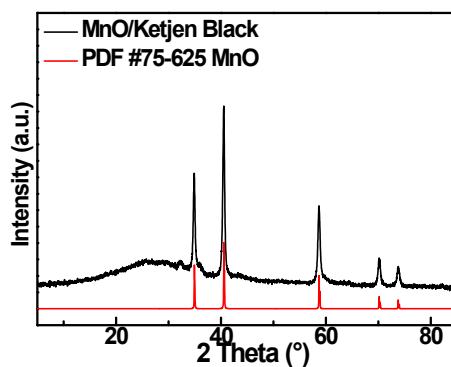


Figure S9. XRD patterns of MnO.

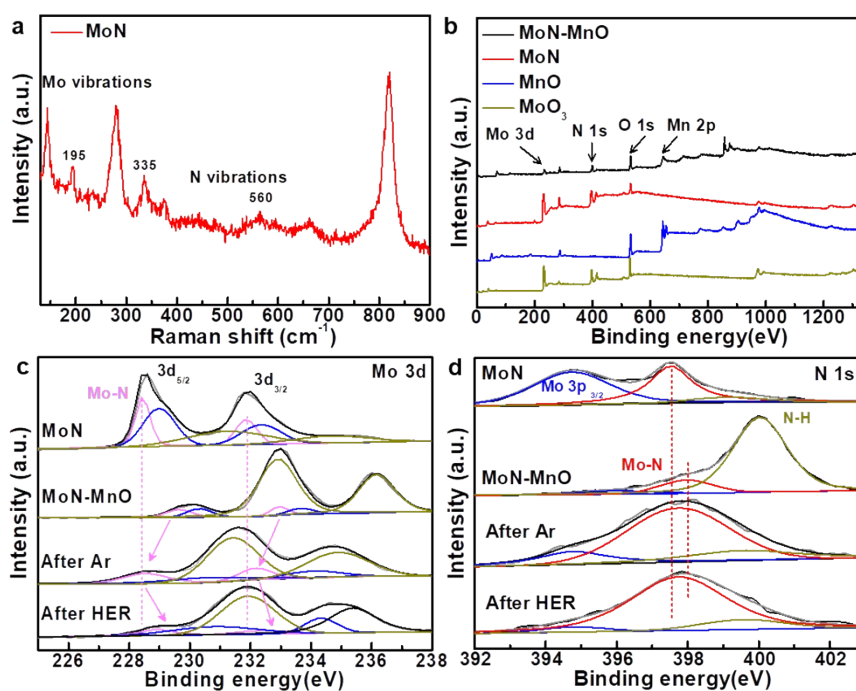


Figure S10. (a) Raman spectra of MoN. (b) XPS survey of the samples. (c) Mo 3d and (d) N 1s spectra of samples.

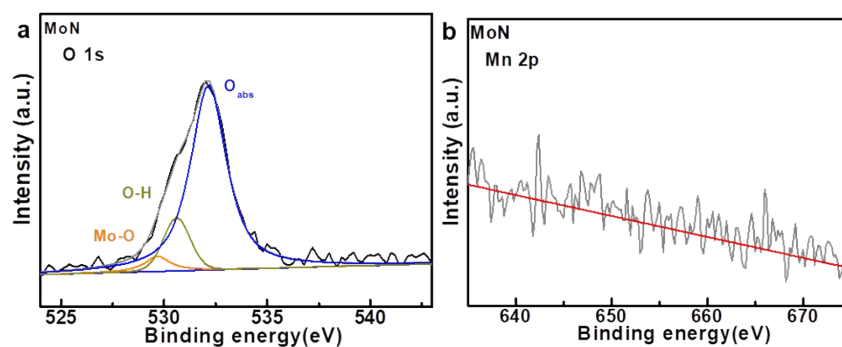


Figure S11. (a) O 1s and (b) Mn 2p XPS spectrum of MoN.

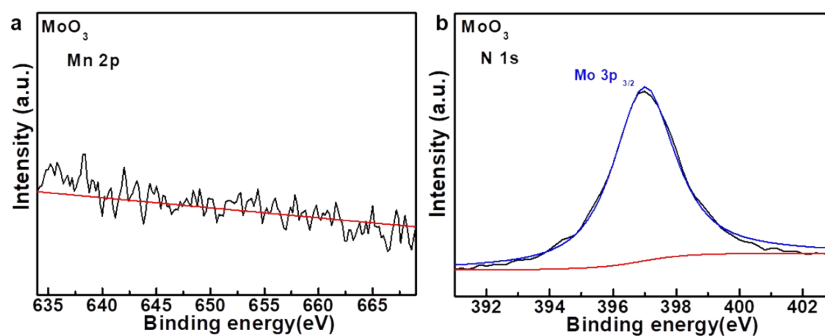


Figure S12. (a) Mn 2p and (b) N 1s XPS spectrum of MoO₃.

The Figure S11 and S12 shows that the Mn is absent in MoN and MoO₃ as the comparisons.

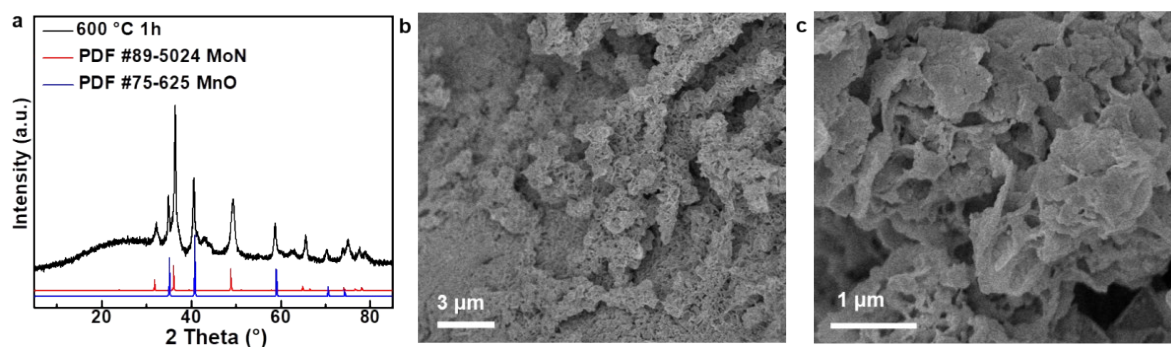


Figure S13. (a) XRD patterns, (b) and (c) SEM image of $\text{Mn}(\text{MoO}_4)(\text{H}_2\text{O})$ calcined in the NH_3 at 600 °C.

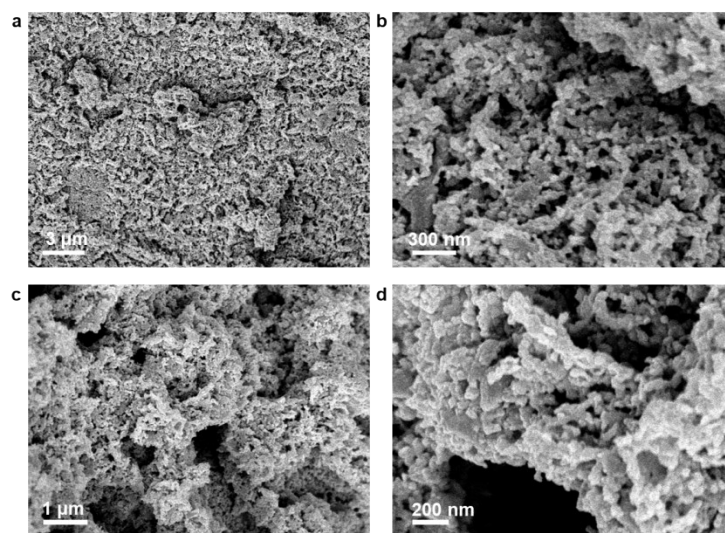


Figure S14. (a) and (b) SEM image of $\text{Mn}(\text{MoO}_4)(\text{H}_2\text{O})$ calcined in the NH_3 at 700 °C. (c) and (d) SEM image of $\text{Mn}(\text{MoO}_4)(\text{H}_2\text{O})$ calcined in the NH_3 at 800 °C.

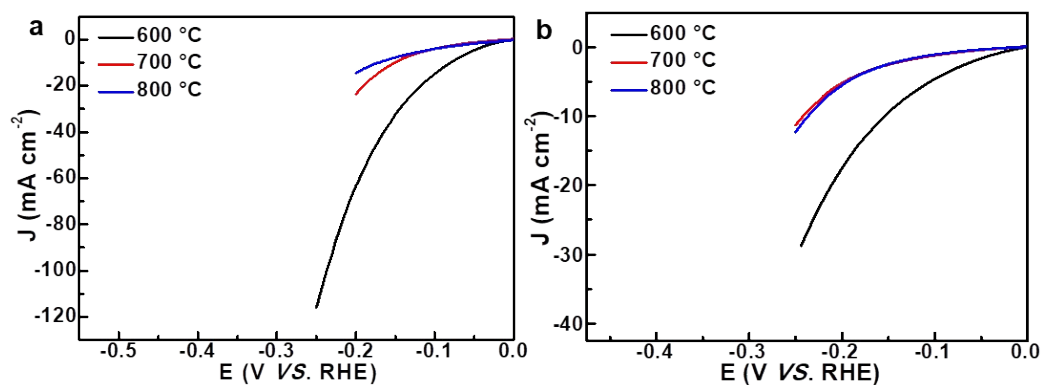


Figure S15. Linear sweep voltammetry (LSV) curves for samples at different temperature in (a) 1.0 M KOH and (b) 1.0 M buffer solution (pH=7.0).

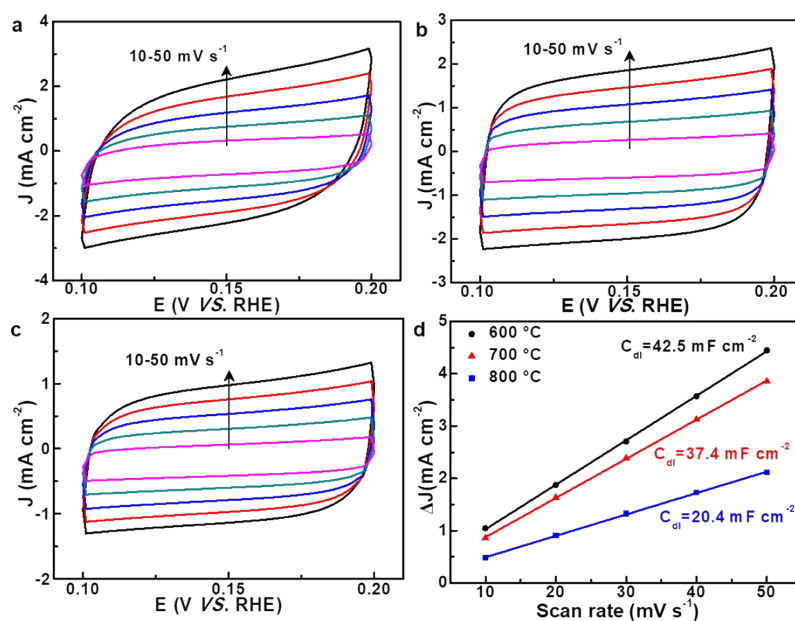


Figure S16. Typical CV curves of (a) 600°C, (b) 700°C and (c) 700°C in 1.0 M KOH with various scan rates, respectively. (d) Corresponding C_{dl} values.

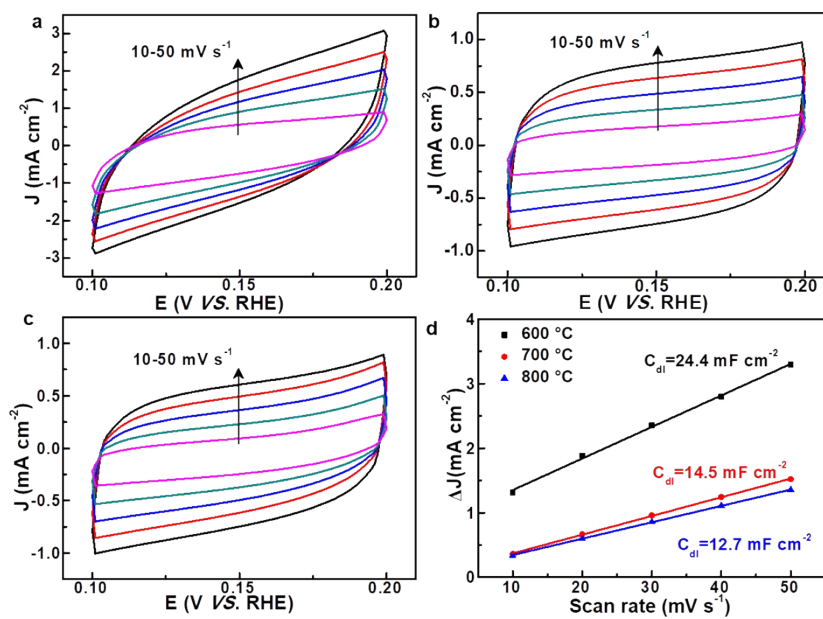


Figure S17. Typical CV curves of (a) 600°C, (b) 700°C and (c) 700°C in 1.0 M buffer solution (pH=7.0) with various scan rates, respectively. (d) Corresponding C_{dl} values.

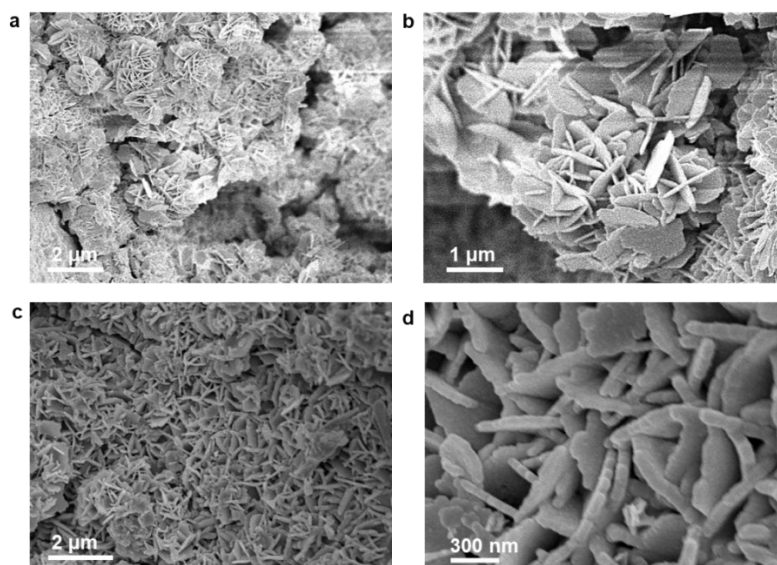


Figure S18. The morphology structure (the mass loading of 2.1 mg cm^{-2}) of (a and b) precursor and (c and d) calcining in the NH_3 at $500 \text{ }^\circ\text{C}$.

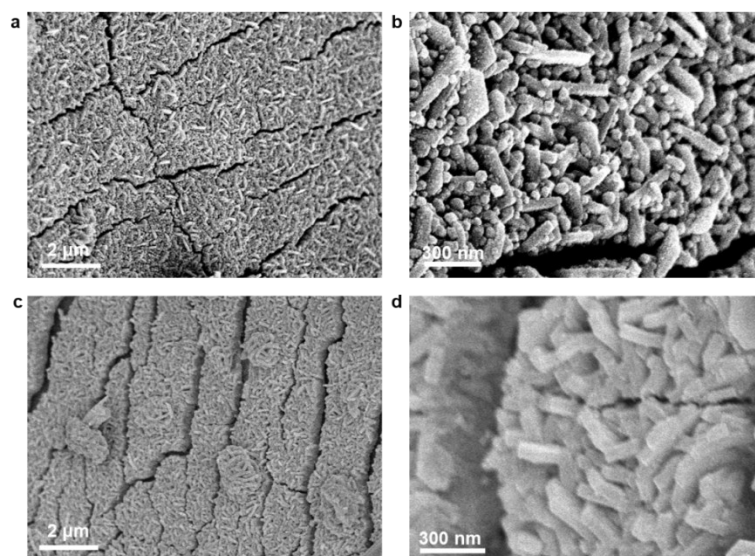


Figure S19. The morphology structure (the mass loading of 2.7 mg cm^{-2}) of (a and b) precursor and (c and d) calcining in the NH_3 at $500 \text{ }^\circ\text{C}$.

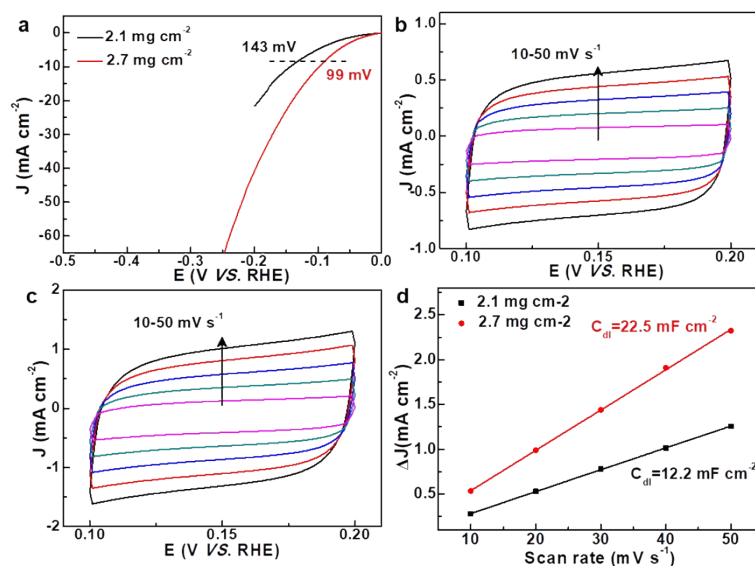


Figure S20. (a) LSV curves for samples of different loading mass. Typical CV curves of the mass loading of (a) 2.1 mg cm⁻² and (b) 2.7 mg cm⁻² in 1.0 M KOH with various scan rates. (d) Corresponding C_{dl} values.

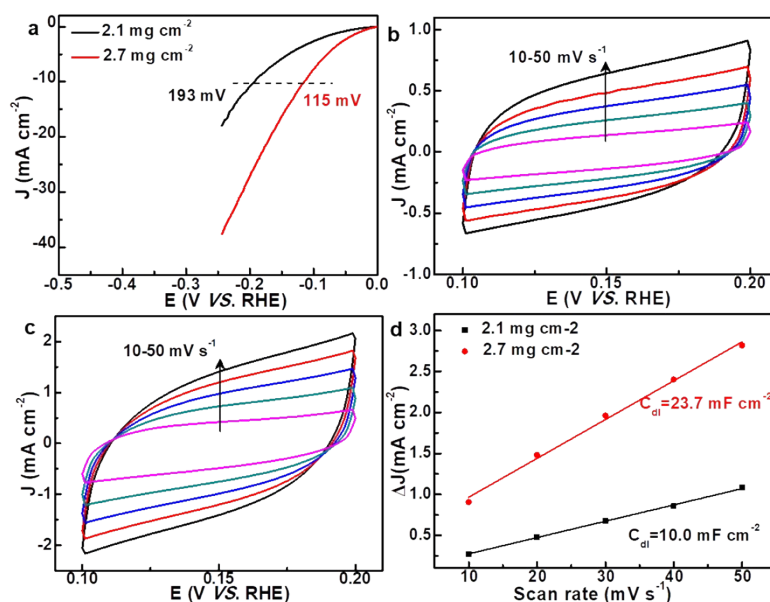


Figure S21. (a) LSV curves for samples of different loading mass. Typical CV curves of the mass loading of (a) 2.1 mg cm⁻² and (b) 2.7 mg cm⁻² in 1.0 M buffer solution (pH=7.0) with various scan rates. (d) Corresponding C_{dl} values.

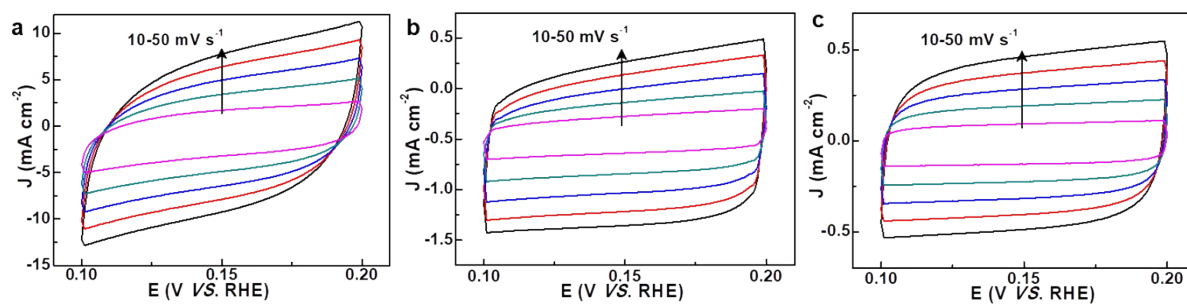


Figure S22. Typical CV curves of (a) MoN-MnO, (b) MoN, and (c) MnO in 1.0 M KOH with various scan rates, respectively.

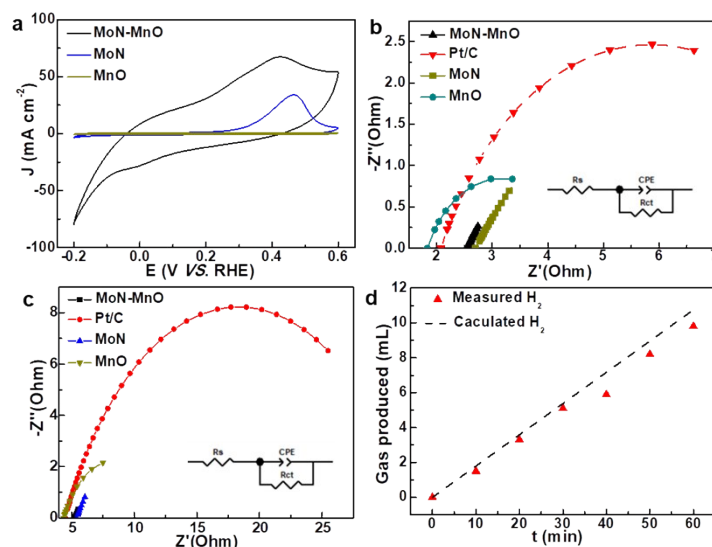


Figure S23. (a) CV curves of MoN-MnO, MoN and MnO in 1.0 M buffer solution (pH=7.0) at a scan rate of 50 mV s⁻¹. Electrochemical impedance spectra of different samples (b) in 1M KOH and (c) 1.0 M buffer solution (pH=7.0), inset: equivalent circuit is used for data analyses, R_s and R_{ct} are the ohmic and charge-transfer resistance, respectively. (d) The Faradaic efficiency of MoN-MnO at constant current density of 10 mA.

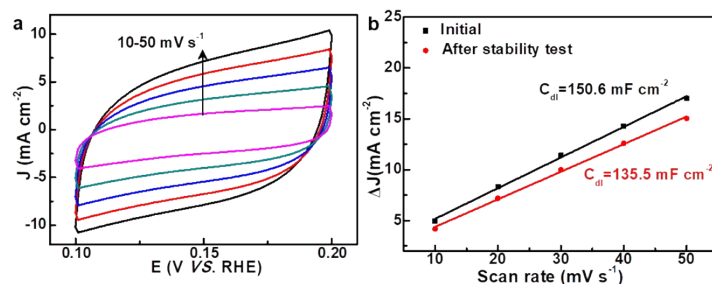


Figure S24. (a) CV curves of MoN-MnO after chronoamperometry measurement at current density of 10 and 50 mA cm⁻² in 1.0 M KOH. (b) Comparison of corresponding C_{dl} values.

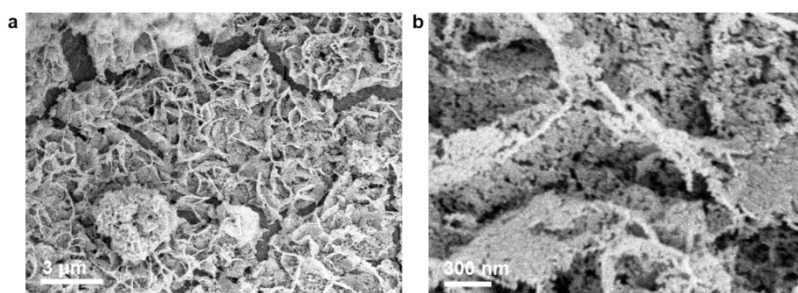


Figure S25. (a and b) SEM image of MoN-MnO after stability test of chronoamperometry at current density of 10 and 50 mA cm⁻² in 1.0 M KOH.

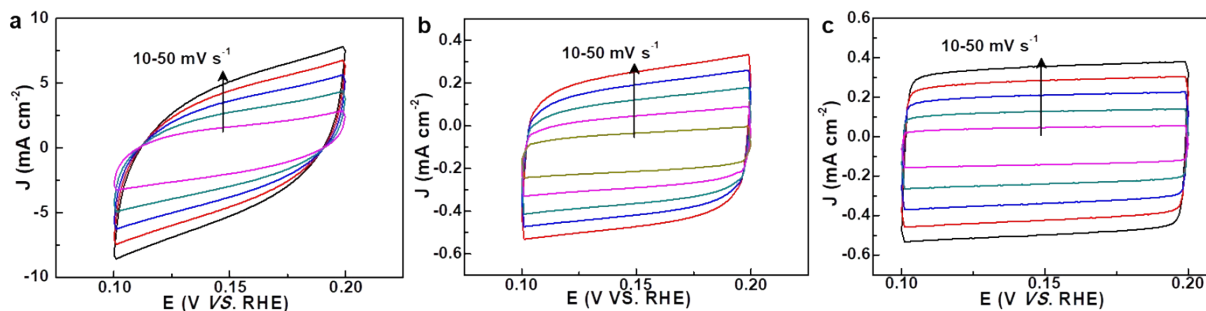


Figure S26. Typical CV curves of (a) MoN-MnO, (b) MoN, and (c) MnO in 1.0 M buffer solution (pH=7.0) with various scan rates, respectively.

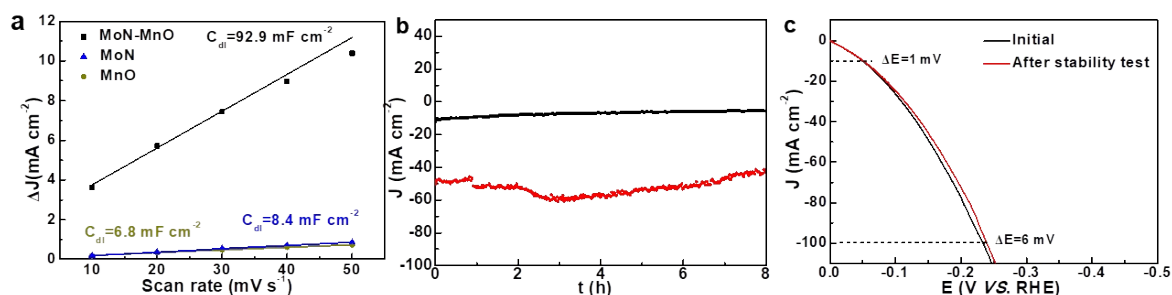


Figure S27. (a) C_{dl} values of MoN-MnO, MoN and MnO in 1.0 M buffer solution (pH=7.0). (b) Chronoamperometric curves at different current densities: 10 and 50 mA cm⁻² in 1.0 M buffer solution (pH=7.0). (c) Comparison HER polarization curves of MoN-MnO after chronoamperometric test.

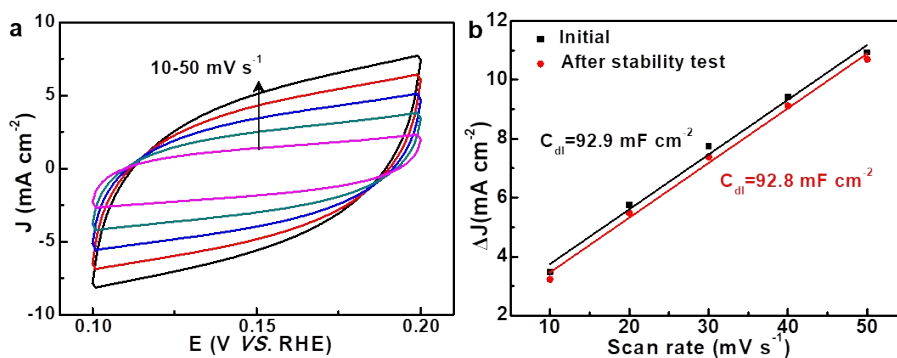


Figure S28. (a) CV curves of MoN-MnO after chronoamperometry measurement at current density of 10 and 50 mA cm⁻² in 1.0 M buffer solution (pH=7.0). (b) Comparison of corresponding C_{dl} values.

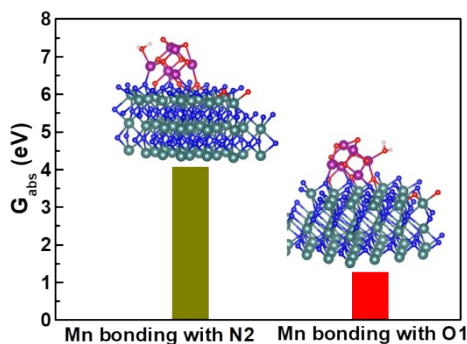


Figure S29. (a) Calculated adsorption energy of water on interface.

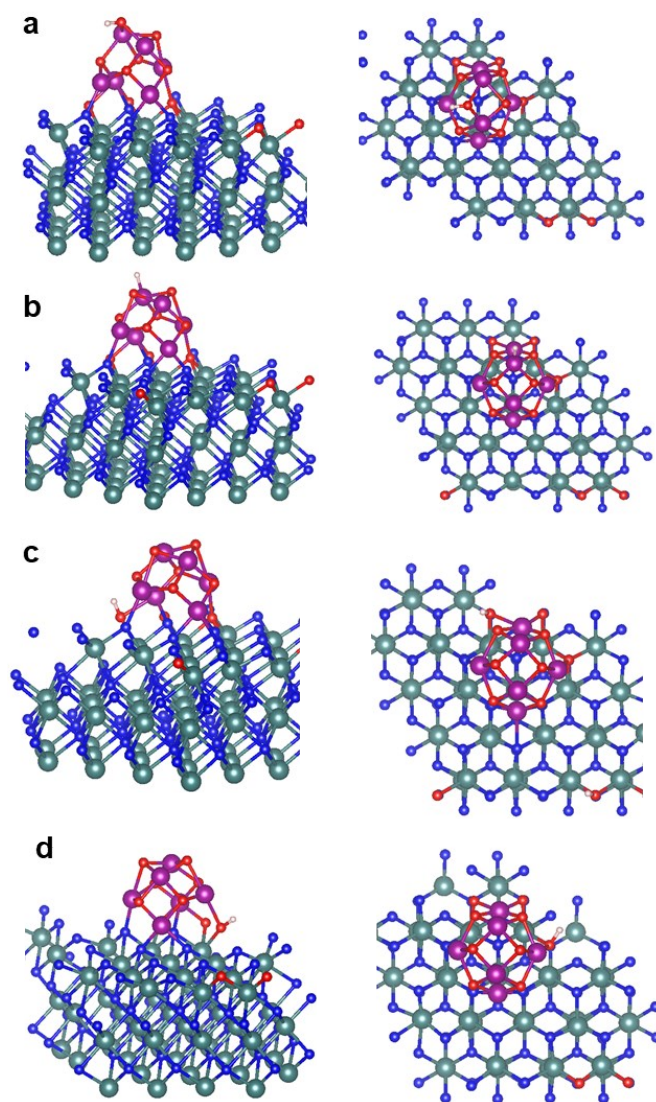


Figure S30. Optimized active sites for H adsorption on Mn-O domains, including (a) O3, (b) Mn1, (c) O2 and (d) O1 sites.

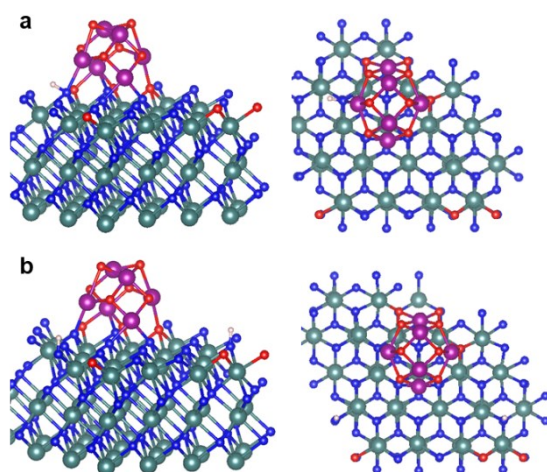


Figure S31. Optimized active sites for H adsorption on MoN domains, including (a) N2 and (b) Nslab sites.

Table S1. Elemental composition of ICP-OES tests.

Mn(MoO₄)(H₂O)		
Element	Mass content (mg cm⁻²)	Mass fraction (%)
Mn	0.32	50.4
Mo	0.56	49.6
MoN-MnO		
Element	Mass content (mg cm⁻²)	Mass fraction (%)
Mn	0.34	48.6
Mo	0.55	51.4

Table S2. The R_{ct} and R_s of electrocatalysis in different solution.

1M KOH		
Catalyst	R_s (Ω)	R_{ct} (Ω)
MoN-MnO	2.56	1.99
Pt/C	2.08	7.56
MoN	2.70	10.71
MnO	1.83	2.66
1M buffer solution		
Catalyst	R_s (Ω)	R_{ct} (Ω)
MoN-MnO	5.26	1.98
Pt/C	4.49	27.69
MoN	5.40	17.73
MnO	4.37	7.74

And internal resistance (R_s) is inevitable, related to electrolytes, electrodes, wires, equipment, etc., which brings about Ohmic potential drop. And it needs further correction in potential–current density (iR-compensation).

References

- 1 H. Jin, X. Liu, A. Vasileff, Y. Jiao, Y. Zhao, Y. Zheng and S.-Z. Qiao, *ACS Nano*, 2018, **12**, 12761-12769.
- 2 W.-B. Luo, S.-L. Chou, W. Jia-Zhao, Y.-C. Zhai and H.-K. Liu, *Sci. Rep.*, 2015, **5**, 8012.

